Supplementary Information

Polydopamine-Based Surface Modification of Novel Nanoparticle-Aptamer Bioconjugates for *In Vivo* Breast Cancer Targeting and Enhanced Therapeutic Effects

Wei Tao[1,2,3*], Xiaowei Zeng[1,2*], Jun Wu[4], Xi Zhu[3], Xinghua Yu[1], Xudong Zhang[5], Jinxie Zhang[1,2], Gan Liu[1,2], Lin Mei[1,2]✉

1. The Shenzhen Key Lab of Gene and Antibody Therapy, and Division of Life and Health Sciences, Graduate School at Shenzhen, Tsinghua University, Shenzhen 518055, P.R. China;
2. School of Life Sciences, Tsinghua University, Beijing 100084, P.R. China.
3. Brigham and Women's Hospital, Harvard Medical School, Boston, Massachusetts 02115, United States.
4. Department of Biomedical Engineering, School of Engineering, Sun Yat-sen University, Guangzhou 510006, P.R. China.
5. Department of Molecular Microbiology and Immunology, University of Southern California, Los Angeles, CA 90033, USA.

* The two authors contributed equally to this work.

✉ Corresponding author: Lin Mei: Tel/Fax: +86 75526036736, E-mail: mei.lin@sz.tsinghua.edu.cn.

Study of pD film growth

The growth of the pD film was further monitored by Malvern Mastersizer 2000 (Zetasizer Nano ZS90, Malvern Instruments Ltd., UK) and a simple equation. In brief, the average size of both pD-NPs at different reaction time (3, 4, 5, 6, 9 and 24 h, n = 10) and bare NPs (n = 10) was evaluated by Malvern Mastersizer. The size of pD film is roughly evaluated by averaging the equation of '(the pD-NP size – the average NP

size)/2'. It can be concluded from the kinetics profile (Supplementary Information, Figure S2) that pD film growth on the DTX/NPs was almost linear during the first 6 h, followed by a slower growth which plateaued at a thickness of ~19 nm after 24 h [1]. Similar results were reported by Lee et al [2].

Evaluation of the affinity of aptamers on NP surface

The affinity of AS1411 aptamers on NP surface was evaluated by a receptor competition assay. The MCF-7 cells were incubated with 1 mM free AS1411 aptamers, drug-free Apt-pD/NPs at the same aptamer concentration (the amount of aptamers on the surface of NPs was calculated in Table S2) or drug-free pD/NPs (at the same NP concentration) for 1 h. The free AS1411 aptamers, drug-free Apt-pD/NPs or drug-free pD/NPs were used as blocking agents. After the blocking procedure, the MCF-7 cells were incubated with 250 μg/ml Apt-pD-C6/NPs for 2 h and stained by DAPI for 10 min. The cell uptake efficiency could be obtained by CLSM images and the quantitative analysis was achieved through ImageJ software.

Due to the amount of aptamers is equal for free aptamers and Apt-pD/NPs, the blocking ability represents for the affinity of aptamers for free aptamers and aptamers on NP surface after getting rid of the blocking influence by pD/NPs. Furthermore, the blocking ability could be evaluated by the cell uptake efficiency, i.e. the locking ability is inversely proportional to the cell uptake efficiency. Thus, the ratio of cell uptake efficiency by "Apt-pD-C6/NPs blocked by free aptamers" and "Apt-pD-C6/NPs blocked by Apt-pD/NPs" is inversely proportional to the ratio of the

average affinity by “free aptamers” and “AS1411 aptamers on the surface of NPs”. As shown in Figure S3, the cell uptake efficiency by “Apt-pD-C6/NPs blocked by free aptamers” is 55.5 %, while the real cell uptake efficiency by“Apt-pD-C6/NPs blocked by Apt-pD/NPs” is 87 % (100 % - 92.6 % + 79.6 %, i.e. getting rid of the blocking influence by pD/NPs). The cell uptake efficiency of “Apt-pD-C6/NPs without blocking” was defined as 100 %. Thus the affinity of aptamers after conjugation on the NP surface falls to 63.8 % of that of free aptamers.

Biocompatibility study of pD film with HEK 293 cells.

To evaluate the biological effect of pD film on normal cells, we conducted a biocompatibility study on HEK 293 cells, a specific cell line originally derived from human embryonic kidney cells. First, the pD-coated glass slides for cells to attach were prepared by incubating the blank glass slides in 0.1 mg/ml dopamine hydrochloride/Tris buffer solution (pH 8.5, dopamine hydrochloride dissolved in a 10 mM Tris buffer) under stirring at room temperature. After magnetic stirring for determined time (i.e. 3 h and 6 h), the mixed solution turned dark slightly and pD film were coated on the glass slides. As shown in Figure S3 (A), the glass slides gradually darken with the increase of incubation time. After high-pressure steam sterilization and drying overnight, the prepared glass slides (bank glass and pD-coated glass) were placed in each well of 6-well tissue culture plates. 2 ml of HEK 293 cells in DMEM medium at a concentration of 2×10^5 cells/ml was added into each well. After incubated in a humidified incubator at 37 °C and 5% CO_2 for 24 h, the attached cells

were observed under an inverted microscope (DMI6000B, LEICA). Furthermore, the HEK 293 cell viability was also evaluated by MTT assays to study the toxicity of pD film. As shown in Figure S3 (B), the pD film seems to be biocompatible and nontoxic to the HEK 293 cells since no obvious cytotoxic activity was observed on pD-coated glasses after 24 and 48 h-incubation. It can be also observed from Figure S3 (C) and (D) that the pD-coated glass slide can have nearly the same good cell adhesion and proliferation status as blank glass slide, further indicating that the pD modification method on NP surface is a safe, nontoxic and promising way to functionalize NPs for biomedical use.

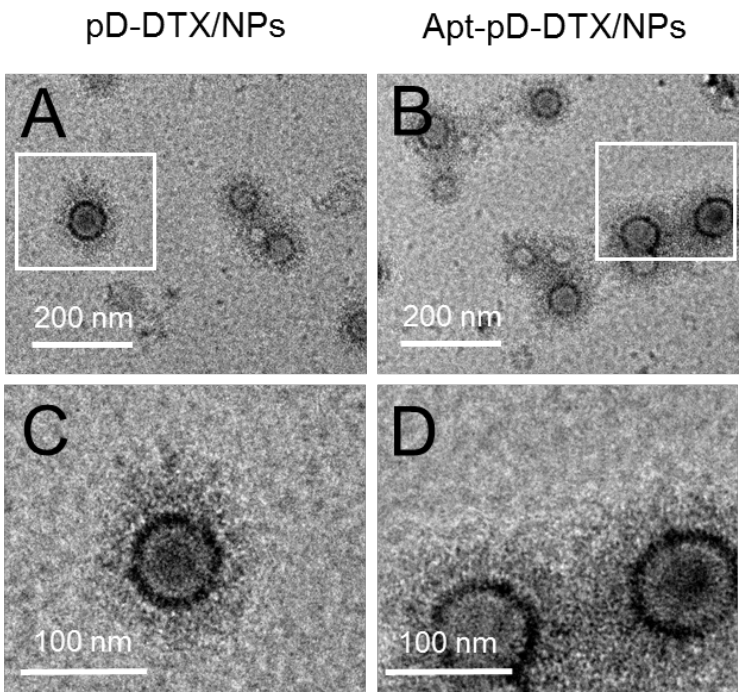

Figure S1. TEM images of (A) pD-DTX/NPs and (B) Apt-pD-DTX/NPs. (C) - (D) Local images in the box are shown in the low panel. The reaction time for pD modification was extended to 6 h in order to thicken the pD film and clearly observe it on the surface of the NPs.

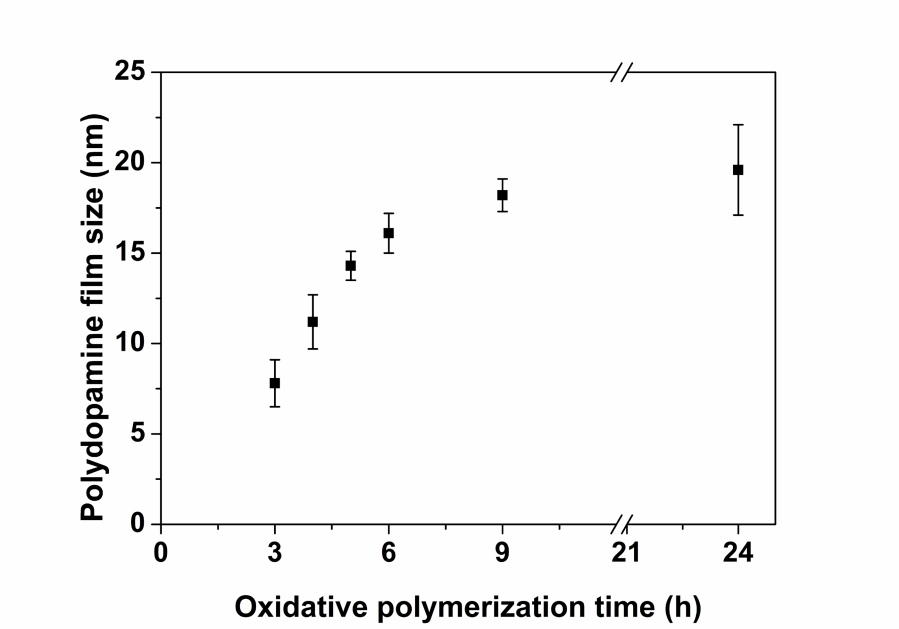

Figure S2. Thickness of polydopamine film as a function of oxidative time (n = 10).

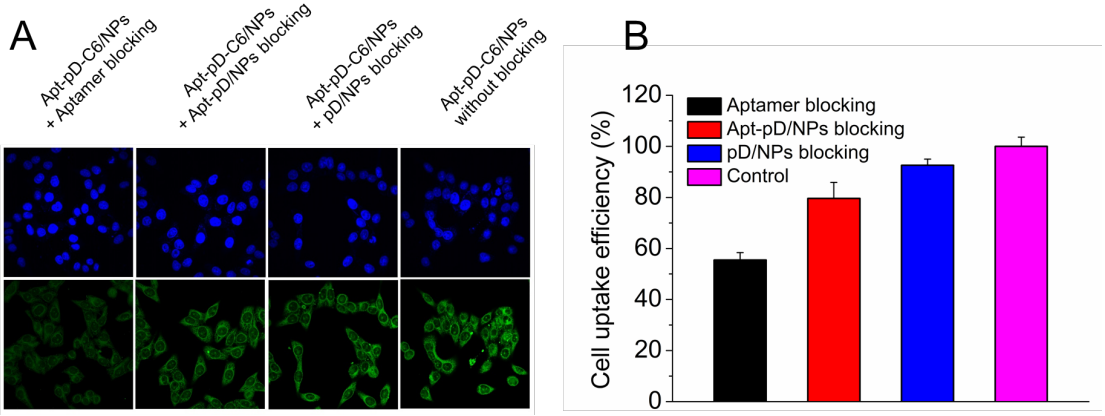

Figure S3. Evaluation of the affinity of AS1411 aptamers on the surface of NPs by a receptor competition assay. (A) CLSM images of MCF-7 cells after 2 h-incubation with Apt-pD-C6/NPs with Aptamer, Apt-pD/NPs or pD/NPs as blocking. The cellular uptake was visualized by overlaying images obtained by EGFP channel (green) and DAPI channel (blue) with the same CLSM parameters and settings. (B) Cell uptake efficiency of Apt-pD-C6/NPs in MCF-7 cells with different blocking agents. The quantitative analysis was achieved through ImageJ, and the fluorescence intensity of Apt-pD-C6/NPs without blocking was defined as 100 %.

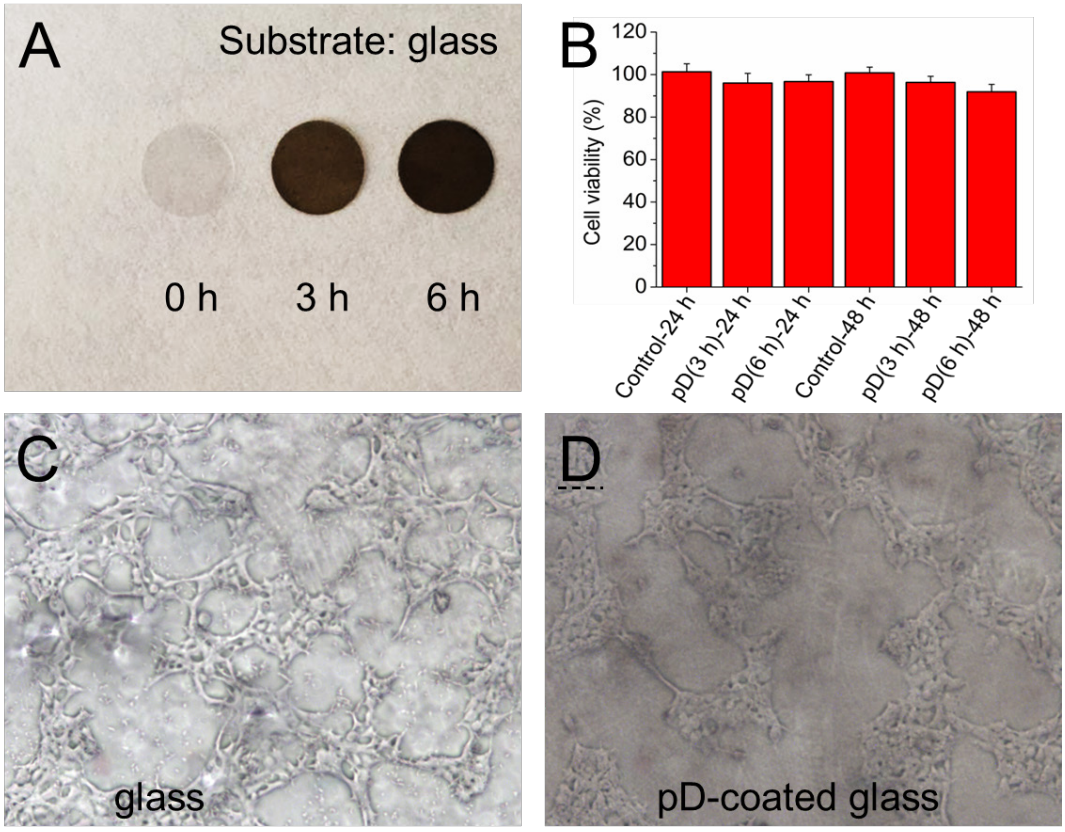

Figure S4. Biocompatibility study of pD film with HEK 293 cells. (A) Multifunctional coating formation by oxidant-induced dopamine polymerization on coverslips (left to right: 0, 3, 6 h after polymerization reaction). (B) Cytotoxicity of pD film detected by MTT assays. Viability of HEK 293 cells cultured on pD film-coated glasses (3 h and 6 h for pD-coating) in comparison with the control group (non-coating) for 24 h and 48 h. (C) Microscopic images of HEK 293 cells on blank glass (i.e. 0 h after polymerization reaction) after 24 h-incubation. (D) Microscopic images of HEK 293 cells on pD-coated glass (3 h for pD-coating) after 24 h-incubation.

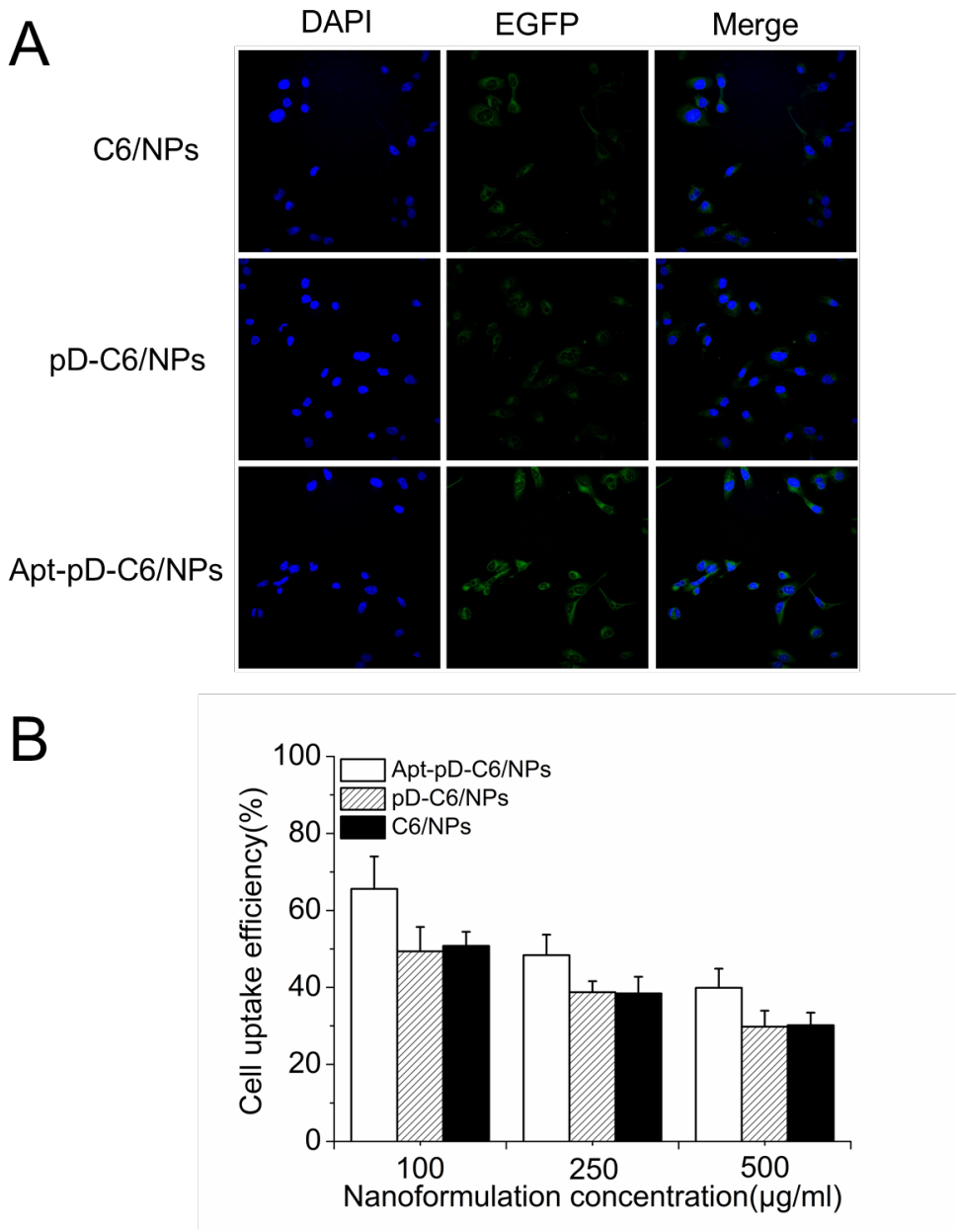

Figure S5. Endocytosis of C6/NPs, pD-C6/NPs and Apt-pD-C6/NPs. (A) CLSM images of MDA-MB-231 cells after 2 h-incubation at 37 °C. (B) Cellular uptake efficiency of C6/NPs, pD-C6/NPs and Apt-pD-C6/NPs in MDA-MB-231 cells after 2 h-incubation at 37 °C.

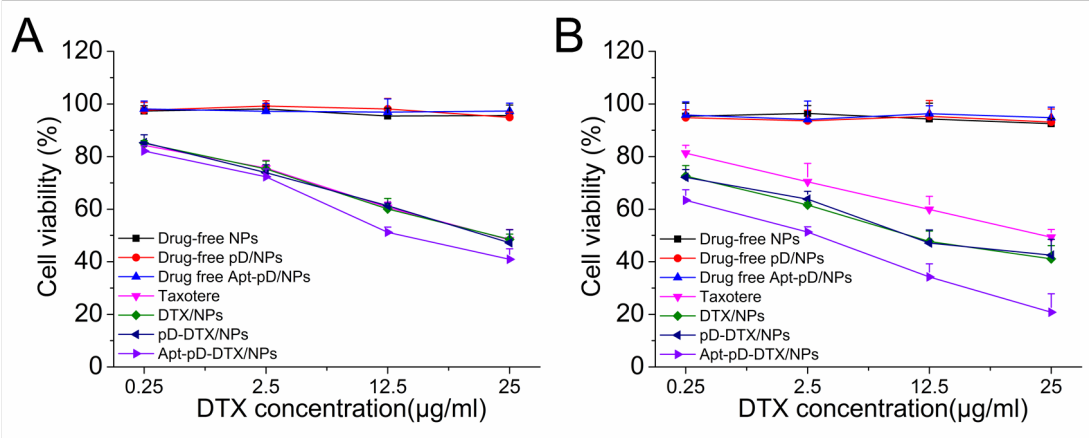

Figure S6. Cytotoxicity of NPs detected by MTT assays. Viability of MDA-MB-231 cells cultured with DTX-loaded NPs in comparison with that of Taxotere® at the same DTX dose and drug-free NPs with the same amount of NPs for (A) 24 h and (B) 48 h.

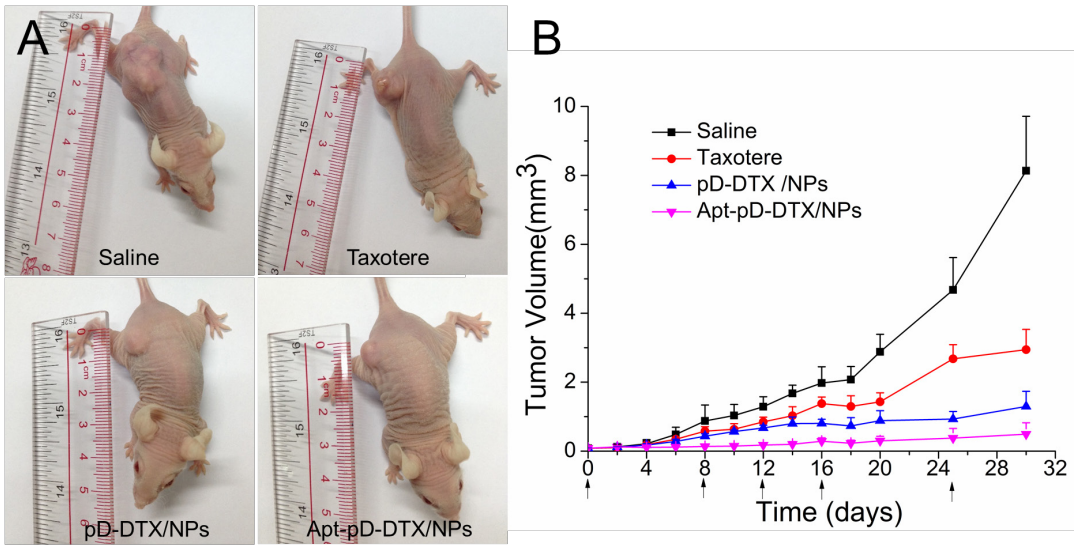

Figure S7. Anti-tumor efficacy of Taxotere®, pD-DTX/NPs, and Apt-pD-DTX/NPs on the SCID nude mice bearing MDA-MB-231 xenograft. (A) Images of tumors in each group on the right back of the nude mice at Day 30. (B) Tumor growth curve after intravenously injected with Saline, Taxotere®, pD-DTX/NPs, and Apt-pD-DTX/NPs.

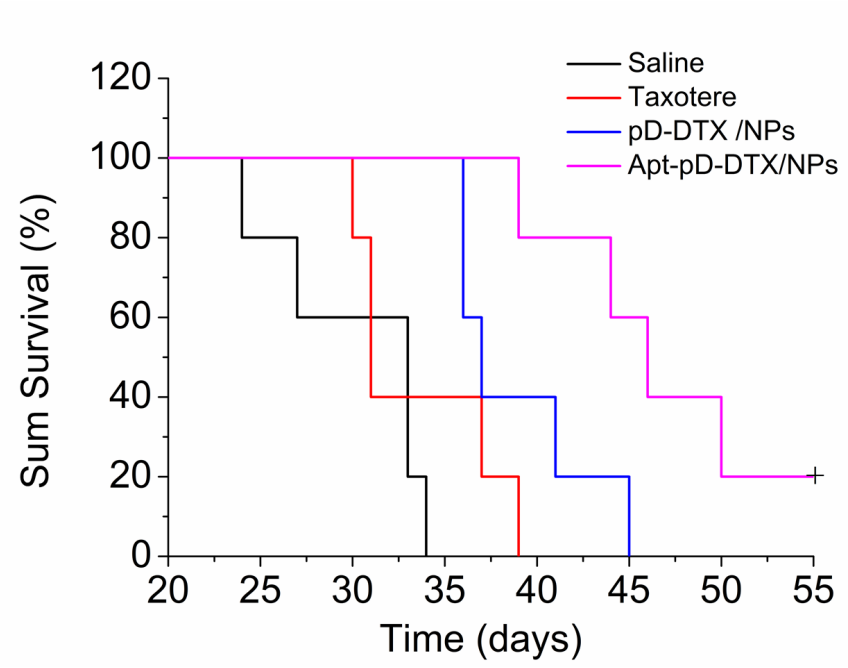

Figure S8. Kaplane-Meier survival log-rank analysis of the TA2 mice bearing breast cancer. The survived time of the animals received Apt-pD-DTX/NPs was significantly longer than that of those received pD-DTX/NPs, Taxotere® and Saline.

References

[1] M. Zhang, X. Zhang, X. He, L. Chen, Y. Zhang, *Nanoscale* **2012**, *4*, 3141-3147.

[2] H. Lee, S. M. Dellatore, W. M. Miller, P. B. Messersmith, *Science* **2007**, *318*, 426-430.

Table S1 Characterization of fluorescent NPs.

Samples (n=3)	Size (nm)	PDI	ZP (mV)
C6/NPs	99.7 ± 3.5	0.121	-13.1 ± 2.9
pD-C6/NPs	107.9 ± 4.6	0.125	-13.7 ± 3.8
Apt-pD-C6/NPs	113.6 ± 5.8	0.107	-14.6 ± 3.6
IR-780/NPs	98.8 ± 4.1	0.113	-12.9 ± 2.7
pD-IR-780/NPs	108.3 ± 4.6	0.129	-13.6 ± 4.5
Apt-pD-IR-780/NPs	112.9 ± 5.1	0.115	-14.1 ± 4.3

PDI = polydispersity index, ZP = zeta potential, n=3

Table S2 Characterization of DTX-loaded NPs redispersed in Tris buffer (TB) and PBS containing 0.1% w/v Tween 80 (PBST).

Samples (n=3)	Size (nm)	PDI	ZP (mV)
DTX/NPs $_{TB}$	101.3 ± 4.1	0.116	-12.8 ± 3.3
pD-DTX/NPs $_{TB}$	109.6 ± 4.3	0.119	-14.3 ± 4.1
Apt-pD-DTX/NPs $_{TB}$	110.3 ± 4.7	0.128	-15.1 ± 3.8
DTX/NPs $_{PBST}$	99.3 ± 3.8	0.120	-12.3 ± 2.9
pD-DTX/NPs $_{PBST}$	109.1 ± 4.2	0.119	-14.1 ± 3.9
Apt-pD-DTX/NPs $_{PBST}$	111.3 ± 4.6	0.123	-14.7 ± 5.2

PDI = polydispersity index, ZP = zeta potential, n=3

Table S3 X-ray photoelectron spectroscopy (XPS) analysis of drug-free NPs, pD/NPs and Apt-pD/NPs.

Samples	XPS elemental ratio (%)		
	C	O	N
NPs	73.62	23.38	-
pD/NPs	69.36	28.29	2.36
Apt-pD/NPs	70.25	26.83	2.92
Samples	Wt (%) of different parts in Apt-pD/NPs from XPS		
	NPs	pD	Apt
Apt-pD/NPs	72.98	25.37	1.65

- Under detection limit.